Catalysis for highly thermostable phenol-terephthalaldehyde polymer networks

Lérys Granado, Romain Tavernier, Gabriel Foyer, Ghislain David, Sylvain Caillol

Catalysis for highly thermostable phenol-terephthalaldehyde networks

Lérys Granado[1*], Romain Tavernier[1], Gabriel Foyer[2], Ghislain David[1], Sylvain Caillol[1]

[1] « Ingénierie et Architecture Macromoléculaire » Institut Charles Gerhardt UMR-5253, CNRS, Université de Montpellier, ENSCM, 40, Avenue Professeur Emile Jeanbrau, 34296 Montpellier, France

[2]ArianeGroup, Rue de Touban, 33185 Le Haillan, France.

*Corresponding author: lerys.granado@live.fr

Abstract

There is a crucial need to eliminate formaldehyde (F) from high-performance thermoset formulations. We propose herein the study of innovative phenol (P)-terephthalaldehyde (TPA) resole, synthesized under basic conditions. For aerospace applications, alkali- or alkaline-earth-based catalysts should be avoided because they degrade the polymer performances in real conditions. To address this issue, we successfully employed DBU to catalyze the resole formation and compared the mechanisms and performances to the usual NaOH-catalyzed formulation. Insights into the undergoing chemical reactions of crosslinking were given by IR and NMR spectroscopies together with thermal analyses (DSC and TGA). We proposed a two-step mechanism pathway, directly arising from the multiple reactions occurring with TPA (compare to only two with F). An in-depth thermo-kinetics study was efficient to compare both NaOH and DBU catalyzed reactions (performed using multiple heating rates DSC data and isoconversional computational method of Vyazovkin). Finally, TGA results showed that these new resoles presented increased thermal performances compare to commercial PF.

TOC

This paper presents innovative and highly-performant phenol-terephthalaldehyde thermosets and gives insights into the catalysis and mechanisms of polymerization.

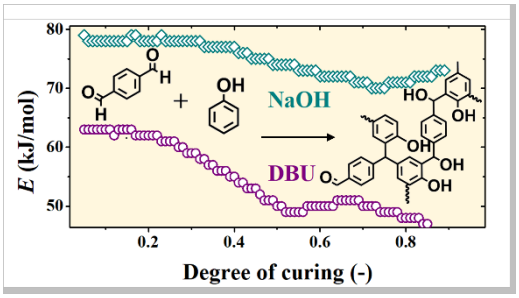

Keywords

Resole; Phenol-Terephthalaldehyde; DBU; Curing Kinetics; Thermal Performances

Introduction

Phenol-formaldehyde (PF) thermosetting polymers were the first plastics industrialized, at the beginning of the 20th century.[1] Phenolic networks are still extensively used in both large-volumes (i.e. construction, wood industry…) and high-performances manufactured goods (aerospace, microelectronics etc.).[2] Especially, their excellent thermal behaviors is due to their highly crosslinked and aromatically dense polymer network structures.[3] This feature makes phenolic thermosets extensively used as binder in ablative composites for rocket thruster manufacturing.[4] However, in these phenolic networks, there is a crucial need to substitute both formaldehyde and phenol monomers which are CMR (carcinogenic, mutagenic and reprotoxic) substances.[5]

Therefore, both academic and industrial scientific communities have done numerous efforts in finding alternative ways to produce high-performances phenolic thermosets free of CMR chemicals.[6–10] Until recently, the replacement of formaldehyde was the most challenging issue for high-performance applications.[11] Indeed, formaldehyde remains the most reactive and the shortest aldehyde monomer, which leads to the most densely crosslinked and aromatic networks,

suited to high-performances. In response, we have proven that terephthalaldehyde (TPA) – a commercially available aromatic dialdehyde which is non-toxic and potentially bio-based,[12,13] can be used as a promising substitute of formaldehyde in resole synthesis (NaOH-catalyzed), even increasing the thermal performances.[14]

However, the use of alkali-metal or alkaline-earth-metal hydroxides should be avoided for applications requiring a high thermal stability, such as ablative resoles for aerospace. Indeed, the hydroxide moieties and the associated cations are known to reduce the oxidative stability and promote water adsorption of the composite materials.[15,16] Yet, alkaline and earth-alkaline hydroxides are very efficient as catalyst in resole. The catalytic action of alkali-metal or alkaline-earth-metal hydroxides has been previously explained by Grenier-Loustalot et al. in the case of phenol-formaldehyde resoles.[17–20] Besides the phenol deprotonation (pK_a ~ 10) which enhances the phenolic positions reactivity, the cation acts as a chelating group; it interacts with phenoxide and aldehyde moieties (Scheme 1b), favoring the *ortho*-additions and enhancing the properties of the cured resoles.[21]

Thus, the scientific and technologic challenge is to replace alkali-metal or alkaline-earth-metal hydroxides catalysts in resole formulation. Earlier, Astarloa-Aierbe *et al.* reported that triethylamine can effectively catalyze the reactions in PF resoles.[22] Therefore, we propose here to study the effect of the catalyst in the phenol-TPA resole formulations which remained to be clarified by substituting NaOH by an amine base. Our preliminary tests showed that the triethylamine was not a sufficiently strong base to effectively catalyze the pre-polymerization reaction (pK_a ~ 11). In addition, the high volatility of triethylamine makes it ill-suited to the thermally activated crosslinking reactions. Thus, we selected a less volatile, with higher pK_a (> 13, in water)[23] amine base: the 1,8-diazabicyclo[5.4.0]undec-7-ene (DBU, Scheme 1c). To the best of our knowledge, this is the first study reporting DBU as an efficient catalyst in resole formulation.

To study the kinetics of a thermally activated process (here the crosslinking reaction), we monitored the reaction by thermal analyses and computed the activation energy.[24] Nowadays, the isoconversional analysis (a model-free kinetic approach) is a minimum required standard in the field.[25] The isoconversional analysis relies on the hypothesis that the temperature scheduled does not modify the reaction pathways.[26] With this analysis, the activation energy is considered variable throughout the thermally-induced process,[27] and it readily provides useful and predictive information on both the kinetics and mechanisms.

In the present investigation, we compared the resole synthesis based on phenol-TPA reaction with NaOH and DBU, as catalysts. We combined spectroscopic measurements – nuclear magnetic resonance (NMR) and middle-infrared absorption (IR) and thermal analyses – differential scanning calorimetry (DSC) and thermogravimetric analysis (TGA) to provide new mechanistic insights, compare their curing behaviors and characterize the polymer performances.

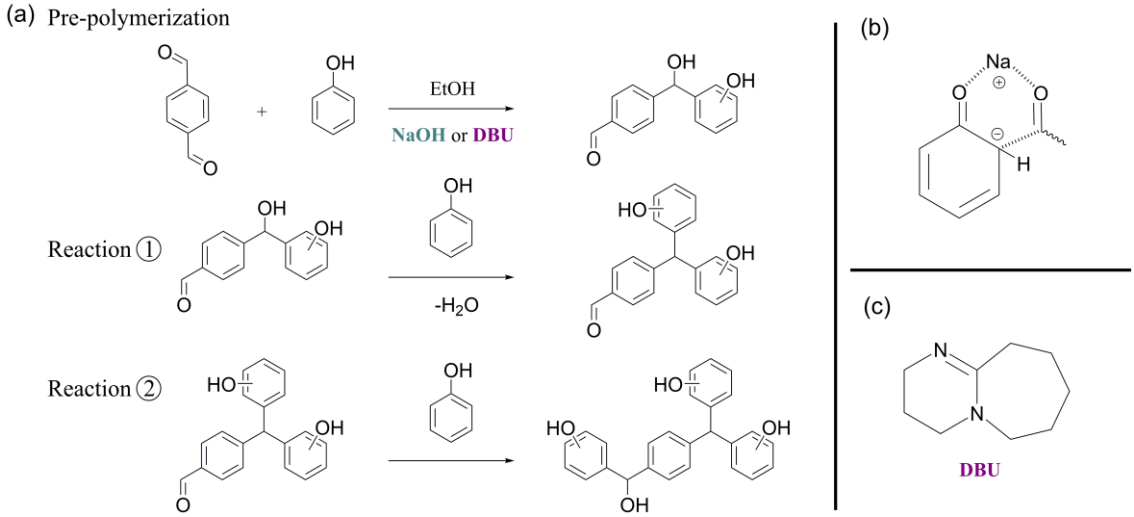

Scheme 1. (a) Mechanism pathway of the reaction between phenol and terephthalaldehyde with the presence of a base, NaOH or DBU. (b) Chelation of methylol and phenoxide by Na^+. (c) Chemical structure of 1,8-diazabicyclo[5.4.0]undec-7-ene (DBU).

Experimental Section

1. Materials

Phenol was purchased from Alfa-Aesar. Terephthalaldehyde and DBU were purchased from TCI Chemicals. Sodium hydroxide and 2,4,6-trimethylphenol (TMP) were purchased from Sigma-Aldrich. Aqueous NaOH solution (50/50, w/w) was freshly prepared using highly pure water. The absolute ethanol was purchased from VWR. Deuterated dimethylsulfoxide (DMSO-d6) was purchased from Eurisotop. The chemicals were at least 98% pure and used without further purification. The liquid prepolymers were stored in a freezer to avoid unwanted reactions.

2. Pre-polymerization

An excess of phenol (in mole, with respect to TPA) and absolute ethanol (< 40 wt.% of the final formulation) were poured in a glass jacketed reactor equipped with a condenser, a glass mechanical stirrer (at 50 rotation per minute) and a circulation bath of ethylene glycol solution regulated at 100.0 ± 0.1 °C. Once the mixture was liquid and homogenous, the TPA was added, the color passed from transparent to orange. After 5 min of homogenization, the catalyst, DBU or aqueous NaOH (< 10 mol.%) were poured in the flask, the color became brownish. The reaction was kept 4 h. Samples were regularly taken off to follow the reaction by IR and ^{1}H NMR. For conversation calculation from NMR spectra, the aldehyde peaks were normalized with respect to the amount of the TMP, as internal reference. After completion of the reaction, the mixture was quenched in an ice bath. In the end, the mixtures were homogeneous, moderately viscous (viscosity < 500 mPa·s) and dark-violet colored. The pre-polymers were used as prepared and studied without any purification.

3. Spectroscopies

The ^{1}H NMR spectra were recorded on a Bruker AC 400 MHz instrument, using deuterated dimethylsulfoxide-d6 as solvent. 4 scans were coadded to each spectrum.

Fourier transform infrared absorption spectroscopy experiments were carried out on a Nicolet 6700 spectrometer from Thermo-Scientific, equipped with a diamond crystal (attenuated total reflectance setup) and a mercury-cadmium-tellurium detector. The spectra were acquired in the middle infrared range, with a resolution of 4 cm^{-1}. 64 scans were coadded to each spectrum.

4. Thermal analyses

The DSC instrument was the DSC-3 F200 Maia (Netzsch GmbH) equipped with an intra-cooler module. The carrier gas was nitrogen (50 $mL \cdot min^{-1}$). The cell sensor was freshly calibrated with biphenyl, indium, bismuth and CsCl standards at 10 $K \cdot min^{-1}$. Between 10 and 12 mg of prepolymer solution was inserted in high-pressure stainless-steel crucibles (Netzsch GmbH, maximum pressure of 100 MPa) to avoid unwanted signal from volatile evaporation. To carry out the non-isothermal kinetics study, the heating rates were: $\beta = \Delta T/\Delta t$ = 5.0, 7.5, 10.0, 12.5 and 15.0 $°C \cdot min^{-1}$. The degree of curing, α, *vs*. temperature at a certain heating rate β_i, was calculated using $\alpha_i(T) = \Delta H_i(T)/\Delta H_{total}$, being the ratio of the released heat $\Delta H_i(T)$ – time integral of the DSC heat flow, using straight baseline, over the total reaction heat (ΔH_{total}) averaged over five measurements.

The TGA experiments were carried out on a TGA-3 libra (Netzsch GmbH). Between 10 and 12 mg of monolithic samples were weighed in open alumina pans. The atmosphere was dried nitrogen at 40 $mL \cdot min^{-1}$. The heating rate was 5 $°C \cdot min^{-1}$ to investigate curing behavior (weight losses due to condensation reaction releasing water). To compare the thermal performances of the cured resole with used the following sequence: 20 $°C \cdot min^{-1}$, from 30 to 900 °C, followed by an isothermal step of 1 h, at 900 °C, to be sure that the char residues were stable.

5. Activation energy computations

The Vyazovkin integral method was used to compute the activation energy values. Theoretical and computational aspects can be found elsewhere.[14] The code was implemented using Python software, using the modules *Scipy* and *Numpy*. Integral functions were calculated using the *scipy.integral.quad* built-in function, with an increment of $\Delta\alpha$ = 0.01. To optimize the computation time (< 1 min), the activation energy in $kJ \cdot mol^{-1}$ is considered as integer values. The results of these computations were consistent with simulated data.

Results and Discussion

1. Prepolymer synthesis and characterization

The conversion during the pre-polymerization is calculated by monitoring the disappearance of the aldehyde NMR signal of the unreacted TPA, near 10.1 ppm (Fig. 1a). The proton of the other aldehyde of the reacted TPA (right-hand side of the top equation on Scheme 1a), is less deshielded near 9.9-10.0 ppm. More than 90% of the second aldehyde for the reacted TPA remains unreacted in either formulation after 4 h. Due to the high aromaticity of these systems,

the protons between 6.7 and 8.2 ppm are mostly overlapped and thus difficult to elucidate. Remarkably, the kinetic profiles displayed in Fig. 1b show that DBU and NaOH lead to identical reaction kinetics, at 100 °C. After 4 h reaction, 95% of the first aldehyde of TPA are reacted in both cases.

The CH protons of the methylenol (secondary alcohols between two rings, i.e. crosslinks) are observed between 5.6 and 6.0 ppm. Compared to previous literature data, the *ortho*- and *para*-positions of the methylenol are assigned to the peaks at 6.1 and 5.7 ppm, respectively (inset Fig. 1a). In the case of the NaOH formulation, the two peak areas are barely similar. There is an equivalent amount of *ortho* and *para* reacted positions (ca. 50% *ortho* / 50% *para*). However, in a phenol there is 2 *ortho* and 1 *para* positions. Thus, even considering the chelating behavior of Na^+ counterions, the *para*-positions are twice more reactive as *ortho* ones. This can be explained by the steric hindrance due to phenoxide in *ortho* positions. For the DBU-catalyzed formulations, the ratio of the phenolic reacted positions is different, 30% *ortho* against 70% *para* (also based on the NMR peak areas). The DBU catalyst enhances the *para*-position reactions. The absence of the chelating counterion with DBU explains the depreciated amount of reacted *ortho*-positions with respect to NaOH.

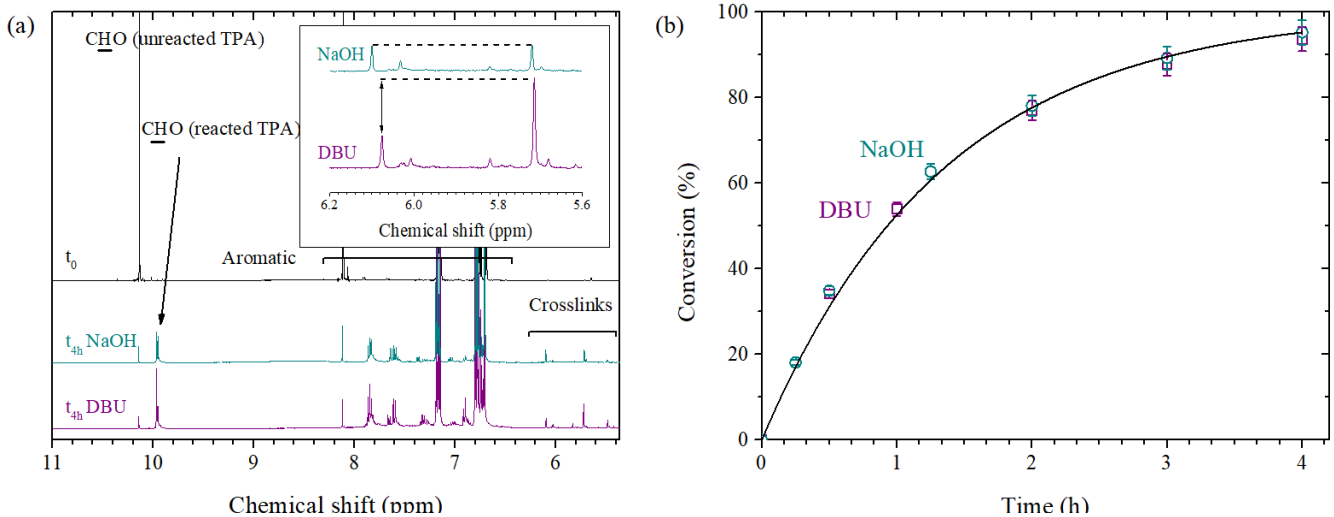

Figure 1. (a) Proton NMR spectra in the region of interest, with taken at t=0 and at t=4h for NaOH and DBU, inset is a magnification showing the protons of methylenol. (b) Kinetic profiles of the pre-polymerization for NaOH and DBU, the error-bars represent the instrumentation uncertainties, they might be smaller than some points. The solid line is an exponential fit, guide of eye.

The IR spectra, in the fingerprint region, recorded during NaOH-catalyzed pre-polymerization are displayed in Fig. 2, and compared to the spectrum of DBU-catalyzed prepolymer (after 4 h reaction). The corresponding IR band assignments are reported in Table 1, in agreement with literature.[28–30] The principal increasing and decreasing bands throughout the pre-polymerization are marked with corresponding arrows. The spectra were normalized with the intensity of the νC-C aromatic band at 1593 cm^{-1}, which is expected to be invariant. One notices the decrease of the νC=O (1683 cm^{-1}) intensity as aldehydes react with phenol. After 4 h reaction, the νC=O band intensity does not reach zero because most of the second aldehyde of TPA remain unreacted. Furthermore, the intensity of the δC-H vibration of phenol (1093 cm^{-1}) decreases as a function of the reaction time, as the results of the electrophilic aromatic substitution. On the other hand, the vibrations of substituted phenol (centered near 1511 and 1602 cm^{-1}) increase, as well as the νC-O (1214 cm^{-1}) and νC-C-O (1110 cm^{-1}) arising from the forming secondary alcohols (methylenol crosslinks), which confirms the structures proposed in NMR. Finally, comparing NaOH- and DBU-catalyzed prepolymers, one barely observes any difference, suggesting similar oligomer structures; except the νC=N (1645 cm^{-1}) vibration caused by DBU. The later vibration intensity was verified to remain constant during the pre-polymerization, confirming that DBU catalyst is neither reacted nor integrated into the polymer network.

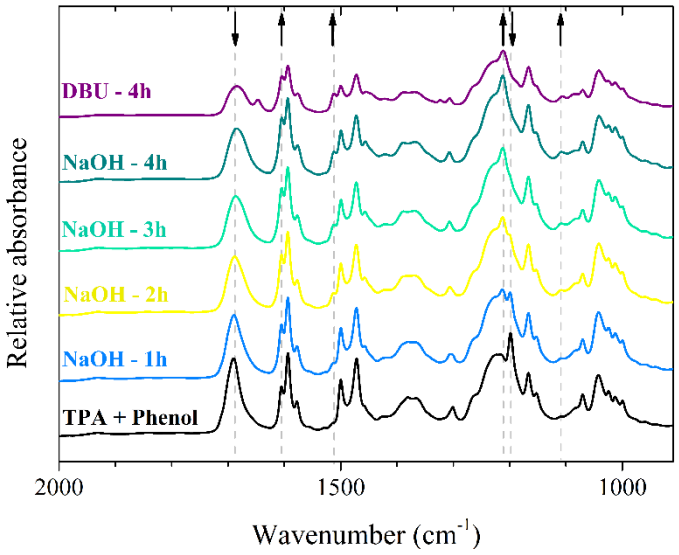

Figure 2. ATR-infrared absorption spectra acquired during the prepolymerization (NaOH and DBU with according points of time written next to the traces). Curve are offset for the sake of clarity. Some varying bands during the prepolymerization are marked with dotted lines and according arrows.

Table 1. Wavenumber at the maximum of some important IR bands, with the probable vibration assignment[28–30] and the associated moieties present in the solution. Star marks the band used as internal reference for spectrum normalization.

Wavenumber (cm^{-1})	Probable vibration assignment	Associated moiety
1683	C=O stretching	Aldehyde
1645	C=N stretching	DBU
1602	Substituted C-C aromatic stretching	Phenyl rings
1593*	C-C aromatic stretching	
1577		
1511	Substituted C-C aromatic stretching	
1453	O-H deformation	Methylenol
1390	In plane C-H rocking	Aldehyde
1308	Not determined	Aromatic aldehyde
1230	C-C-OH phenolic stretching	Phenol
1214	C-O stretching	Methylenol
1168	Interaction of O-H deformation and C-O stretching vibration	Phenol
1110	C-C-O stretching	Methylenol
1093	In plane C-H deformation	Phenol
1071	C-C-O stretching	Ethanol

2. Crosslinking mechanisms

To clarify the crosslinking mechanisms, we compared thermal analyses to IR spectroscopic data (with NaOH formulation). First, we performed non-isothermal curing by DSC. The DSC thermograms in Fig. 3 shows a two overlapped exothermic peak, which suggests a two-fold mechanism pathway. The two reactions are highlighted by the peak deconvolution (Gaussian functions). At 5 °C·min^{-1}, the first reaction (1) starts at 110 °C and ends at ca. 220 °C. The second reaction (2) is triggered around 170 °C and lasts until 260-280 °C. We can define a mixed regime (1) + (2), in which both reaction occurs concomitantly (ca. 170-220 °C). TGA thermogram, also acquired at 5 °C·min^{-1}, shows the weight loss occurring during the cure (open pan). For $T \leq 130$ °C, the weight losses are assigned to volatile evaporation, such as free phenol and solvent. Then, the further weight losses are supposed to come from the condensation reaction releasing water, for $T > 130$ °C. As matter of fact, we observe that the curve plateaus concomitantly with the

end of the reaction (1). Thus, we assume that the reaction (1) involves condensation reactions, whereas the reaction (2) does not. By deepening the analyses, we performed IR spectra on samples that have been pre-cured within the DSC crucibles at 5 °C·min^{-1} until a certain extent, and then quenched rapidly (at - 40 °C·min^{-1}) to room temperature. The scatter dots linked – to the tertiary axis on Fig. 3 – represent the aldehyde content (relative intensity of the νC=O vibration normalized to the intensity before pre-curing). Each point represents independent samples. Interestingly, the aldehyde content is more or less constant during the reaction (1) and as far as the reaction (2) is not triggered. When the reaction (2) starts, we observe a significant and remarkably linear decay of aldehyde content.

If we summarize, the deconvolution of DSC thermograms shows that a two-step crosslinking mechanism occurs in the non-isothermal curing of these resoles. The reaction (1) comprises weight losses and no consumption of aldehyde moieties. On the other hand, the reaction (2) does not involve any weight loss and the aldehyde actually reacts. These strong evidences allow us to propose the mechanism depicted in Scheme 1a. During the prepolymerization, only the first aldehyde of the TPA reacts with phenol to create methylenol bridges. Then, during curing, the first reaction (1) would be the condensation of this methylenol with phenol, releasing water. And finally, the reaction (2) involves the addition of phenol onto the dangling aldehydes (second CHO moiety of TPA) which remained unreacted, so far. Finally, the condensation of the secondly formed methylenol would mostly occur at a very small extent, due to the lack of remaining reactive phenolic positions.

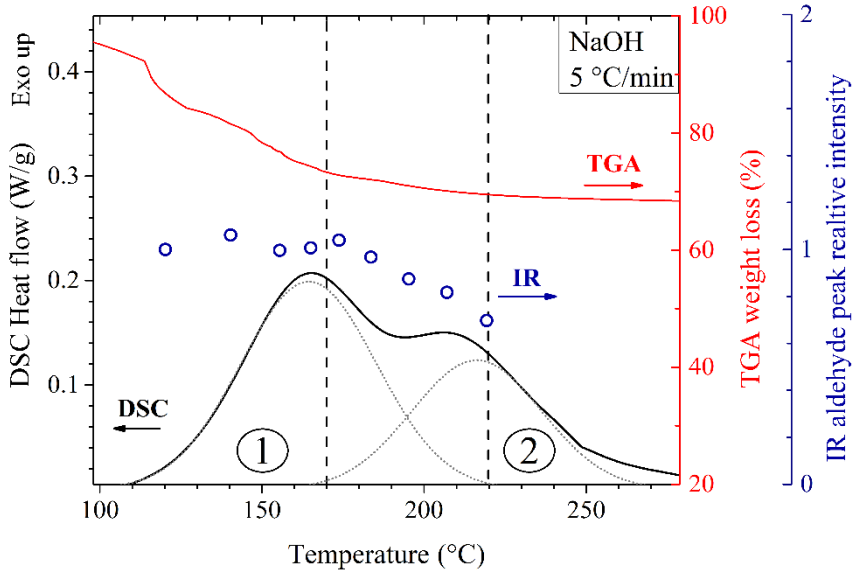

Figure 3. DSC thermograms of NaOH-catalyzed curing, recorded at 5 °C·min^{-1} with a peak deconvolution into two Gaussian contributions (dotted lines), primary axis, TGA thermograms recorded during curing of NaOH formulation at 5 °C·min^{-1} (secondary axis), and relative intensity of the IR vibration of νC=O (at 1683 cm^{-1}), normalized with the according IR intensity of the uncured NaOH prepolymer (I =1 for α = 0), tertiary axis. The zone between the dotted lines is the mixed regime (1) + (2).

3. Thermo-kinetics of curing

The DSC thermograms recorded at multiple heating rates are depicted in Fig. 4ab, showing the heat flow against the temperature during the exothermic curing process. The curves exhibit similar shapes for both formulations. The two peaks observed in both NaOH and DBU catalyzed curing are assigned to reactions (1) and (2), at lower and higher temperatures respectively. Remarkably, the first peak for both formulations occurs within the same temperature range, for all heating rates, e.g. peak maxima of 186 °C at 15 °C·min^{-1}. However, the second reaction is shifted to higher temperature for DBU at the same heating rate (peak maxima of 231 and 264 °C for NaOH and DBU, respectively). It supposedly hardly remains free *para*-position in DBU formulations, and due to the lack of the chelating counterion, the kinetics of the reaction (2) are slowed compared to NaOH (which benefited from more available *para*-positions and enhanced reactivity of *ortho*-positions). The total heat of reaction (i.e. enthalpy) is almost identical for NaOH and

DBU catalyzed processes (204 ± 5 and 198 ± 14 J·g^{-1} respectively). This suggests that the same amount of crosslink is obtained in all cases. If the total reaction heat is calculated regarding the amount of phenol in formulation, the value is nearly 10 kJ·mol^{-1} of phenol.

After integration of the thermograms, the non-isothermal kinetic profiles are displayed in Fig. 4cd. The sigmoidal shapes are very typical of thermoset curing processes. Yet, due to the multi-step mechanisms of the process, slope breaks are observed at $\alpha \sim 0.5$. The fact that the slope breaks are all consistently recorded at the same conversion is a condition of applicability of the isoconversional analysis (i.e. the temperature schedule does not affect the mechanisms). The sigmoid-shaped curves are parallel for most of the cases (except at extreme high degrees of curing, where integration errors are more prominent). The presented data are therefore considered well suited to isoconversional analysis to compute activation energy values. One can readily observes that the kinetic profiles are sparser for DBU than for NaOH.

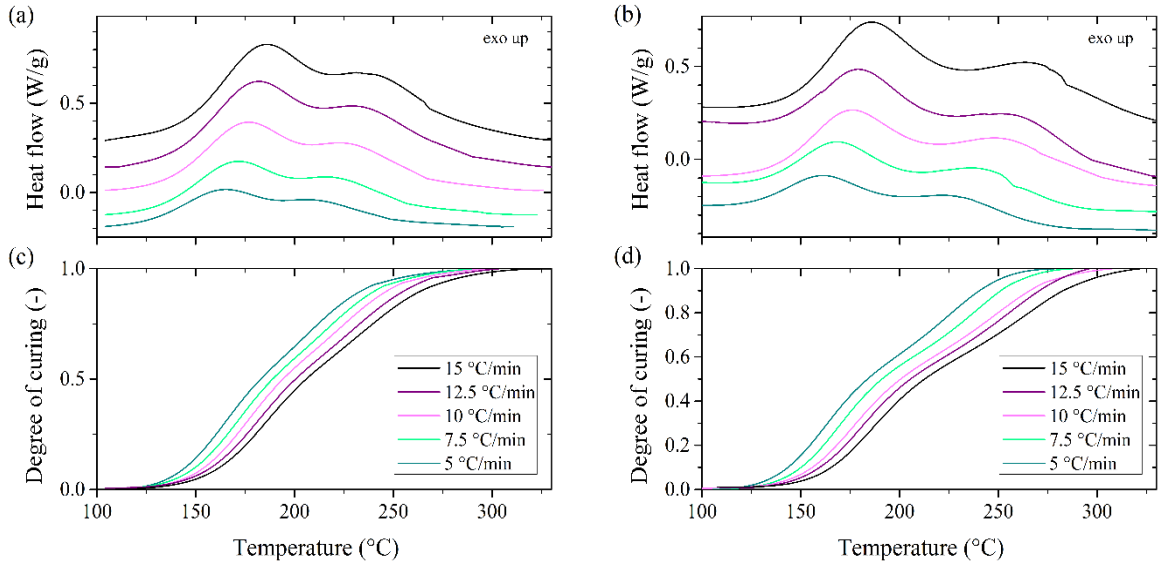

Figure 4. Non-isothermal DSC thermograms at different heating rates, for NaOH (a) and DBU (b) catalyzed formulations (stacked and offset curves). (c) NaOH and (d) DBU, non-isothermal kinetic profiles according to the thermograms. See online version for colored curves.

The isoconversional analysis assumes that the temperature (T) and the conversion (α) are independent variables, thus using an empirical Arrhenius equation, we have:

$$\frac{\mathrm{d}\alpha}{\mathrm{d}t} = A\,\mathrm{e}^{-\frac{E}{\mathrm{RT}(t)}} \times f(\alpha) \qquad \text{Equation 1}$$

where, dα/dt is the reaction rate (which is here the ratio of the DSC heat flow over ΔH_{total}), A the pre-exponential factor, E the activation energy, R the gas constant, $\beta = T/\Delta t$, and f the model sum-function. Following the isoconversional analysis hypothesis, and setting $f(\alpha)$ constant for α = constant, we have the fundamental expression of the isoconversional analysis:

$$\left[\frac{\partial \ln(d\alpha/dt)}{\partial T^{-1}}\right]_\alpha = \left[\frac{\partial \ln(A\exp(-E/RT))}{\partial T^{-1}}\right]_\alpha + \left[\frac{\partial \ln(f(\alpha))}{\partial T^{-1}}\right]_\alpha = -\frac{E_\alpha}{R} \qquad \text{Equation 2}$$

where E_α is the isoconversional value of the activation energy, *i.e.* the activation energy associated to one value of α. The Vyazovkin method is based on the eq. (2) and writes:

$$\min[\Phi(E_\alpha)] = \sum_{i=1}^{n}\sum_{j\neq i}\frac{J_i(E_\alpha,T_{\alpha,i})}{J_j(E_\alpha,T_{\alpha,j})} \qquad \text{Equation 3}$$

where n is the number of probed temperature programs (here n = 5) and $J_i(E_\alpha, T_{\alpha,i})$ is the time integral of the i$^{\text{th}}$-temperature program $T_i(t)$, as:

$$J_i(E_\alpha, T_{\alpha,i}) = \int_{t_{\alpha-\Delta\alpha}}^{t_\alpha} e^{-\frac{E_\alpha}{RT_{\alpha,i}(t)}} \cdot dt \qquad \text{Equation 4}$$

with an iterative process, E_α values are found being the solution of the minimum of Φ, for each isoconversional value, α, with small increments (usually $\Delta\alpha = 0.01$).

The activation energy values are computed using Vyazovkin method from the integral experimental dataset (i.e. kinetic profiles) for both formulations (Fig. 5). E_α spans over a wide range of values, from ca. 50 to 80 kJ·mol^{-1}. Such high dispersity is also observed on previous kinetic results of PF curing in the literature.[31–35] The two curves display similar shapes, suggesting analogous mechanism pathways. After a first plateau zone (1), the activation energy decreases with α with a remarkable linearity (linear regressions: $R^2 > 0.99$), zone (1) + (2), prior to level-off (2). The deviations from a plateau on the later cases are assumed to be originated from experimental and integration errors. During the first plateau, the activation energy is associated to the reaction (1), E_1 – Scheme 1a. Averaging the values, we found $E_1^{NaOH} = 78 \pm 1$ kJ·mol^{-1} and $E_1^{DBU} = 63 \pm 1$ kJ·mol^{-1}. The zone (1) + (2) is a mixed regime where both reactions are concomitant. The zone (2) is ascribed to the reaction (2), writing E_2 the associated activation energy, we have $E_2^{NaOH} = 72 \pm 2$ kJ·mol^{-1} and $E_2^{DBU} = 49 \pm 3$ kJ·mol^{-1}. One notes that the lower activation energy values for DBU were expected due to the more scattered kinetic profiles in Fig. 2d, in comparison with NaOH (Fig. 2c).

The reasons of such decrease in activation energy when using DBU instead of NaOH remain to be clarified. Earlier, Gabilondo *et al.* remarked similar trends: triethylamine catalyzed PF resole presented lower energy than NaOH catalyzed ones.[31] However, the mechanistic explanation based on vitrification/gelation contribution to the activation energy were not satisfactory, in our sense. Indeed, in our case, we notice the absence of the diffusion contribution to the activation energy (which usually tend to significantly higher E with increasing α, in comparison, for instance, to epoxy cured PF novolac)[36]. The reactive sites are located on short monomers in the case of phenolic resins, therefore the polymer network does not hinder the curing kinetics with additional diffusion barriers. Rather, one can be hypothesized that due to less steric hindrance, the *para*-position reactive group (more represented in DBU formulation) would display a lower activation energy (i.e. supposedly, less energetic transition states) than its *ortho* counterpart, tending to lower the overall activation energy values (theoretical computations would be of a precious help to verify this hypothesis). Moreover, the shifts from the reaction mechanisms are different for both formulation (dotted lines, Fig. 3). The shift from reaction (1) to the mixed regime (1) + (2), occurs at $\alpha \sim 0.3$ for NaOH and 0.2 for DBU. The shift from the mixed regime (1) + (2) to strict reaction (2) at $\alpha \sim 0.7$ for NaOH against 0.5 for DBU. This shows that the reaction (2) is more prominent in the case of NaOH than for DBU, and vice versa.

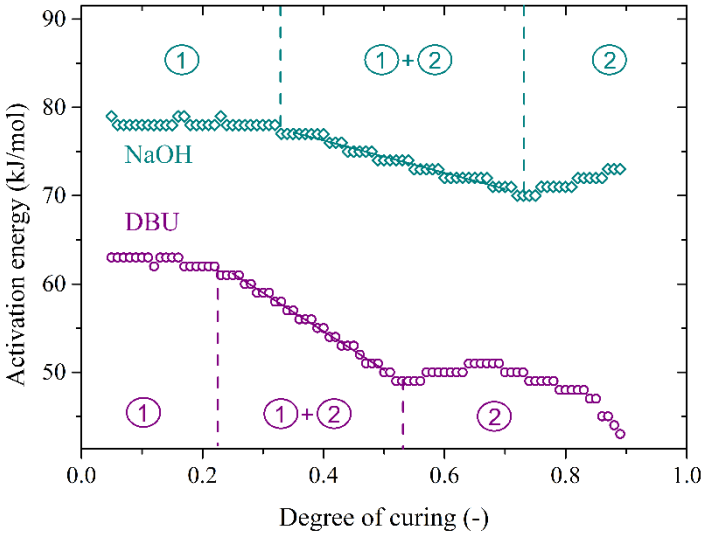

Figure 5. Activation energy values vs. degree of curing, as computed with Vyazovkin method for NaOH and DBU formulations. Dotted lines highlight the change in mechanisms. Solid lines are linear regressions within the mixed regimes ($R^2 > 0.99$).

4. Polymer performances

To avoid the presence of bubbles (polycondensation crosslinking), we performed the curing step within a pressurized autoclave. The solid contents after full curing, at 200 °C for 6 h, are reported in Table 2, i.e. mass after full curing and volatile evaporation (ethanol, free phenol, water), are good in all formulations, and rather close to the theoretical values (72 wt.%). The perfect insolubility in acetone shows that the cured networks are fully crosslinked and chemically resistant (they are also perfectly resistant to ethanol, aqueous sodium hydroxide (1 mol L^{-1}) and tetrahydrofuran).

To evaluate the thermal performance, monolithic and bubble-free cured samples were analyzed using TGA, under pyrolysis conditions. Furthermore, we compared the thermal resistance to a commercial high-performances PF resole currently used in the aerospace industry. The TGA thermograms of all resoles are rather similar (Fig. 6). For T < 400 °C the slight weight losses (< 10 wt.%) are assigned to remaining volatiles evaporation which were trapped into the networks.[37–40] Then, for higher temperatures, the weight losses are assigned to first, the crosslinks degradation and then to ring dehydrogenation forming the amorphous residual char.[37–40] One notes that the curves level-off near 700-800 °C which means that the char residues are stable under these pyrolysis conditions (only 1 wt.% loss was recorded on a subsequent isothermal step at 900 °C, not showed here). The temperature at 10% of degradation is around 400°C for both formulations, showing a high thermal stability. The char yield is slightly higher for NaOH formulation (69 wt.%) than for DBU (64 wt.%). One probable explanation is the higher amount of *ortho*-position with NaOH catalyzed formulations. Overall, the thermal resistances of both formulations are excellent and undoubtedly overtake the high-performance commercial PF resole. They are therefore well-suited to aerospace applications.

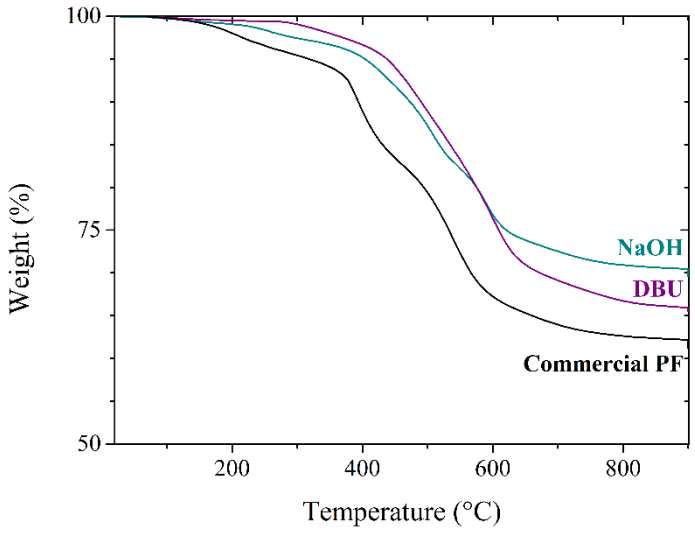

Figure 6. TGA thermograms of the thermal decomposition of the NaOH and DBU based phenol-TPA resole and compared to a commercial PF, under pyrolysis conditions, at 20 °C·min^{-1}.

Table 2. Recapitulating table of the results of NaOH and DBU based phenol-TPA resole (errors are one standard deviation)

Properties / Formulations	NaOH	DBU
Prepolymer viscosity (mPa·s)[a]	470 ± 20	280 ± 5
Solid content (%)[b]	69 ± 1	64 ± 1
Insoluble fraction (%)[c]	99 ± 1	99 ± 1
Char yield at 900 °C (wt.%)	69 ± 1	64 ± 1

[a] Measured at 25 °C on an AR-1000 rheometer (TA instrument) with a 25 mm diameter and 4° cone-plan geometry, flow mode a gradient from 700 to 10 s^{-1}, values are the average value over 10 points and one standard-deviation as errors.
[b] Mass ratio after full curing at 200 °C for 6 h with respect to prepolymer mass.
[c] Mass ratio after 24 h of immersion in acetone at room temperature and drying 24 h at 60 °C.
Errors represent one standard-deviation.

Conclusions

This paper gives interesting insights in the effect of the catalyst involved in the resole synthesis from terephthalaldehyde and phenol which role remained to be clarified. We compared two formulations containing either NaOH or DBU as catalyst, which were processed in the same conditions. We proved, for the first time, that DBU can

catalyze the resole synthesis and curing. The DBU was shown to catalyze reactions on *ortho*-position at a fewer extent than NaOH, due to the absence of a chelating cation. From non-isothermal DSC data and Vyazovkin isoconversional method, we evaluated the curing kinetics. In either case, the curing kinetics showed analogous two-step mechanisms, which were conversion-dependent. The activation energy values of DBU formulation were 10 to 20 $kJ \cdot mol^{-1}$ lower than NaOH ones. Finally, the cured networks were found to present very good performances, such as chemical and thermal resistances, which make them well-suited to high-performance applications.

Acknowledgments

The authors acknowledge Claire Negrell for experimental support and Mélanie Decostanzi for fruitful discussions.

Conflict of Interest

There is no conflict to declare.

References

(1) Hirano, K.; Asami, M. Phenolic Resins-100 Years of Progress and Their Future. *Reactive and Functional Polymers*. 2013, pp 256–269.

(2) Pilato, L. Phenolic Resins: 100Years and Still Going Strong. *React. Funct. Polym.* **2013**, *73* (2), 270–277.

(3) Pizzi, A.; Ibeh, C. C. Phenol–Formaldehydes. In *Handbook of Thermoset Plastics*; Elsevier, 2014; pp 13–44.

(4) Natali, M.; Kenny, J. M.; Torre, L. Science and Technology of Polymeric Ablative Materials for Thermal Protection Systems and Propulsion Devices: A Review. *Progress in Materials Science*. 2016, pp 192–275.

(5) European Chemical Agency. *Annex VI of Regulation (EC) No 1272/2008 (CLP Regulation)*; 2015.

(6) Li, J.; Zhang, J.; Zhang, S.; Gao, Q.; Li, J.; Zhang, W. Fast Curing Bio-Based Phenolic Resins via Lignin Demethylated under Mild Reaction Condition. *Polymers (Basel).* **2017**, *9* (9).

(7) Li, J.; Wang, W.; Zhang, S.; Gao, Q.; Zhang, W.; Li, J. Preparation and Characterization of Lignin Demethylated at Atmospheric Pressure and Its Application in Fast Curing Biobased Phenolic Resins. *RSC Adv.* **2016**, *6* (71), 67435–67443.

(8) Van Gils, G. E. Reaction of Resorcinol and Formaldehyde in Latex Adhesives for Tire Cords. *Ind. Eng. Chem. Prod. Res. Dev.* **1968**, *7* (2), 151–154.

(9) Pizzi, A.; Scharfetter, H. O. The Chemistry and Development of Tannin/Urea–formaldehyde Condensates for Exterior Wood Adhesives. *J. Appl. Polym. Sci.* **1979**, *23* (9), 2777–2792.

(10) Badhe, Y.; Balasubramanian, K. Novel Hybrid Ablative Composites of Resorcinol Formaldehyde as Thermal Protection Systems for Re-Entry Vehicles. *RSC Adv.* **2014**, *4* (55), 28956–28963.

(11) Foyer, G.; Chanfi, B. H.; Virieux, D.; David, G.; Caillol, S. Aromatic Dialdehyde Precursors from Lignin Derivatives for the Synthesis of Formaldehyde-Free and High Char Yield Phenolic Resins. *Eur. Polym. J.* **2016**, *77*, 65–74.

(12) Brindell, G. D.; Lillwitz, L. D.; Wuskell, J. P.; Dunlop, A. P. Polymer Applications of Some Terephthalaldehyde Derivatives. *Ind. Eng. Chem. Prod. Res. Dev.* **1976**, *15* (1), 83–88.

(13) Qin, Z. zeng; Su, T. ming; Jiang, Y. xiu; Ji, H. bing; Qin, W. guo. Preparation of W-Modified FeMo Catalyst and Its Applications in the Selective Oxidization of p-Xylene to Terephthalaldehyde. *Chem. Eng. J.* **2014**, *242*, 414–421.

(14) Granado, L.; Tavernier, R.; Foyer, G.; David, G.; Caillol, S. Comparative Curing Kinetics Study of High Char Yield Formaldehyde- and Terephthalaldehyde-Phenolic Thermosets. *Thermochim. Acta* **2018**.

(15) Sanoj, P.; Kandasubramanian, B. Hybrid Carbon-Carbon Ablative Composites for Thermal Protection in Aerospace. *J. Compos.* **2014**, *2014*, 1–15.

(16) Pilato, L. A.; Michno, M. J. *Advanced Composite Materials*; Springer Berlin Heidelberg: Berlin, Heidelberg, 1994.

(17) Grenier-Loustalot, M. F.; Larroque, S.; Grenier, P.; Leca, J. P.; Bedel, D. Phenolic Resins: 1. Mechanisms and Kinetics of Phenol and of the First Polycondensates towards Formaldehyde in Solution. *Polymer (Guildf).* **1994**, *35* (14), 3046–3054.

(18) Grenier-Loustalot, M. F.; Larroque, S.; Grande, D.; Grenier, P.; Bedel, D. Phenolic Resins: 2. Influence of Catalyst Type on Reaction Mechanisms and Kinetics. *Polymer*. 1996, pp 1363–1369.

(19) Grenier-Loustalot, M. F.; Larroque, S.; Grenier, P.; Bedel, D. Phenolic Resins: 3. Study of the Reactivity of the Initial

Monomers towards Formaldehyde at Constant PH, Temperature and Catalyst Type. *Polymer (Guildf).* **1996**, *37* (6), 939–953.

(20) Grenier-Loustalot, M. F.; Larroque, S.; Grenier, P.; Bedel, D. Phenolic Resins: 4. Self-Condensation of Methylolphenols in Formaldehyde-Free Media. *Polymer (Guildf).* **1996**, *37* (6), 955–964.

(21) Yi, Z.; Zhang, J.; Zhang, S.; Gao, Q.; Li, J.; Zhang, W. Synthesis and Mechanism of Metal-Mediated Polymerization of Phenolic Resins. *Polymers (Basel).* **2016**, *8* (5).

(22) Astarloa Aierbe, G.; Echeverría, J. M.; Riccardi, C. C.; Mondragon, I. Influence of the Temperature on the Formation of a Phenolic Resol Resin Catalyzed with Amine. *Polymer (Guildf).* **2002**, *43* (8), 2239–2243.

(23) Kaupmees, K.; Trummal, A.; Leito, I. Basicities of Strong Bases in Water: A Computational Study. *Croat. Chem. Acta* **2014**, *87* (4), 385–395.

(24) Vyazovkin, S.; Chrissafis, K.; Di Lorenzo, M. L.; Koga, N.; Pijolat, M.; Roduit, B.; Sbirrazzuoli, N.; Suñol, J. J. ICTAC Kinetics Committee Recommendations for Collecting Experimental Thermal Analysis Data for Kinetic Computations. *Thermochim. Acta* **2014**, *590*, 1–23.

(25) Vyazovkin, S.; Burnham, A. K.; Criado, J. M.; Pérez-Maqueda, L. A.; Popescu, C.; Sbirrazzuoli, N. ICTAC Kinetics Committee Recommendations for Performing Kinetic Computations on Thermal Analysis Data. *Thermochim. Acta* **2011**, *520* (1–2), 1–19.

(26) Simon, P. ISOCONVERSIONAL METHODS Fundamentals, Meaning and Application. *J. Therm. Anal. Calorim.* **2004**, *76*, 123–132.

(27) Vyazovkin, S. A Time to Search: Finding the Meaning of Variable Activation Energy. *Phys. Chem. Chem. Phys.* **2016**, *18* (28), 18643–18656.

(28) Long, D. A. *Infrared and Raman Characteristic Group Frequencies. Tables and ChartsGeorge Socrates John Wiley and Sons, Ltd, Chichester, Third Edition, 2001. Price £135*; 2004; Vol. 35.

(29) Tejado, A.; Peña, C.; Labidi, J.; Echeverria, J. M.; Mondragon, I. Physico-Chemical Characterization of Lignins from Different Sources for Use in Phenol-Formaldehyde Resin Synthesis. *Bioresour. Technol.* **2007**, *98* (8), 1655–1663.

(30) Gabilondo, N.; Martín, M. D.; Mondragon, I.; Echeverría, J. M. Polymerization of Formaldehyde and Phenol at Different Pressures. *High Perform. Polym.* **2002**, *14* (4).

(31) Gabilondo, N.; López, M.; Ramos, J. A.; Echeverría, J. M.; Mondragon, I. Curing Kinetics of Amine and Sodium Hydroxide Catalyzed Phenol-Formaldehyde Resins. *Journal of Thermal Analysis and Calorimetry*. 2007, pp 229–236.

(32) He, G.; Riedl, B.; Aït-Kadi, A. Curing Process of Powdered Phenol-Formaldehyde Resol Resins and the Role of Water in the Curing Systems. *Journal of Applied Polymer Science*. 2003, pp 1371–1378.

(33) Wang, J.; Laborie, M. P. G.; Wolcott, M. P. Comparison of Model-Free Kinetic Methods for Modeling the Cure Kinetics of Commercial Phenol-Formaldehyde Resins. *Thermochim. Acta* **2005**, *439* (1–2), 68–73.

(34) Lei, Y.; Wu, Q. Cure Kinetics of Aqueous Phenol-Formaldehyde Resins Used for Oriented Strandboard Manufacturing: Effect of Wood Flour. *J. Appl. Polym. Sci.* **2006**, *102* (4), 3774–3781.

(35) Rivero, G.; Pettarin, V.; Vázquez, A.; Manfredi, L. B. Curing Kinetics of a Furan Resin and Its Nanocomposites. *Thermochim. Acta* **2011**, *516* (1–2), 79–87.

(36) Granado, L.; Kempa, S.; Gregoriades, L. J.; Brüning, F.; Genix, A. C.; Fréty, N.; Anglaret, E. Kinetic Regimes in the Curing Process of Epoxy-Phenol Composites. *Thermochim. Acta* **2018**.

(37) Bessire, B. K.; Minton, T. K. Decomposition of Phenolic Impregnated Carbon Ablator (PICA) as a Function of Temperature and Heating Rate. *ACS Appl. Mater. Interfaces* **2017**, *9* (25), 21422–21437.

(38) Bessire, B. K.; Lahankar, S. A.; Minton, T. K. Pyrolysis of Phenolic Impregnated Carbon Ablator (PICA). *ACS Appl. Mater. Interfaces* **2015**, *7* (3), 1383–1395.

(39) Jackson, W. M.; Conley, R. T. High Temperature Oxidative Degradation of Phenol–formaldehyde Polycondensates. *J. Appl. Polym. Sci.* **1964**, *8* (5), 2163–2193.

(40) Jiang, H.; Wang, J.; Wu, S.; Yuan, Z.; Hu, Z.; Wu, R.; Liu, Q. The Pyrolysis Mechanism of Phenol Formaldehyde Resin. *Polym. Degrad. Stab.* **2012**, *97* (8), 1527–1533.